S45F-0378

Nature of Deep Earthquakes in the Pacific Plate from Unsupervised Machine Learning

Gilbert Mao[1,2], Thomas P. Ferrand[3,4], Jiaqi Li[1,5], Brian Zhu[1,6], Ziyi Xi[1] and Min Chen[1,7]

(1) Department of Computational Mathematics, Science and Engineering, Michigan State University, East Lansing, MI 48824, USA; (2) William Mason High School, Mason, OH, 45040, USA; (3) Institute of Geological Sciences, Freie Universität Berlin, 12249 Berlin, Germany; (4) Institut des Sciences de la Terre d'Orléans, UMR-7327, Université d'Orléans – CNRS, Orléans, France; (5) Department of Earth, Planetary, and Space Sciences, University of California, Los Angeles, CA 90095, USA; (6) Department of Statistics and Data Science, Yale University, New Haven, CT 06520, USA; (7) Department of Earth and Environmental Sciences, Michigan State University, East Lansing, MI 48824, USA

INTRODUCTION

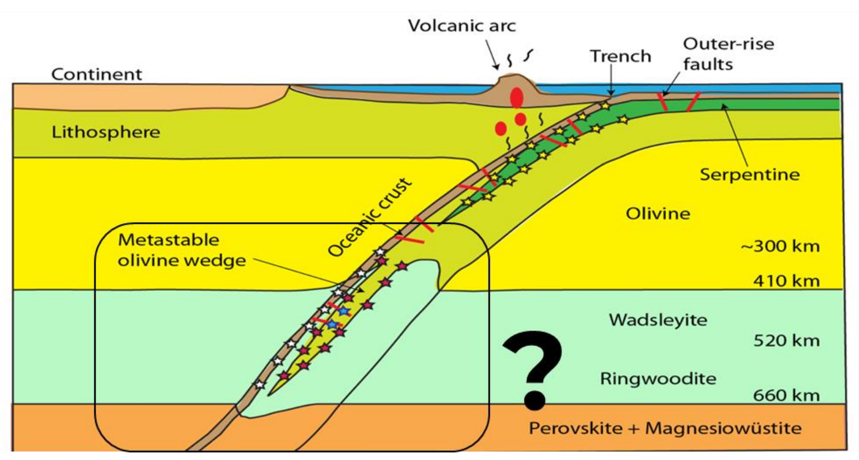

1. thermal shear instability
2. dehydration embrittlement
3. transformational faulting

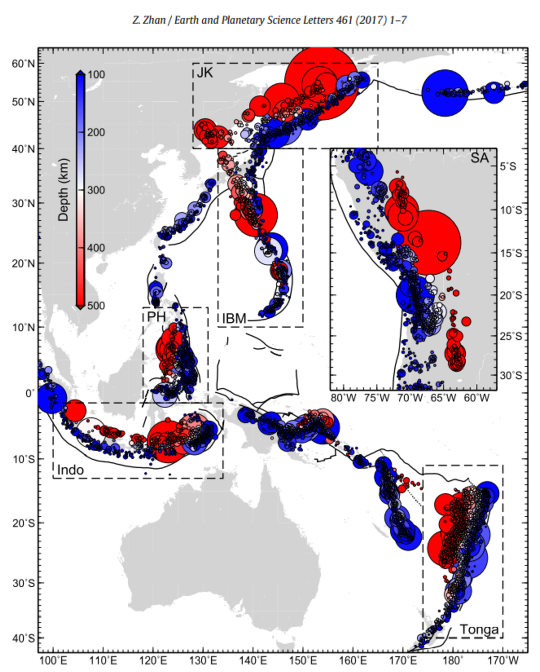

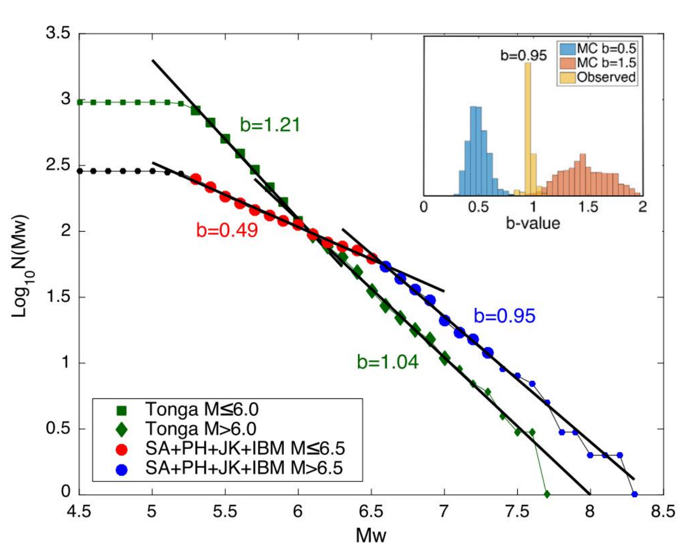

Previous b-value Kink Observed at Mw 6.5 in Certain Subduction Zones.

Dual Mechanism Hypothesis Based on b-value Analysis of CMT Catalog

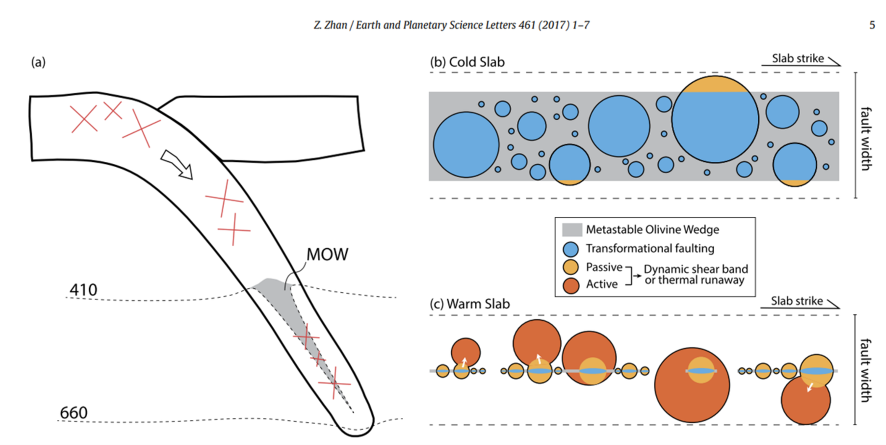

Data & Analysis

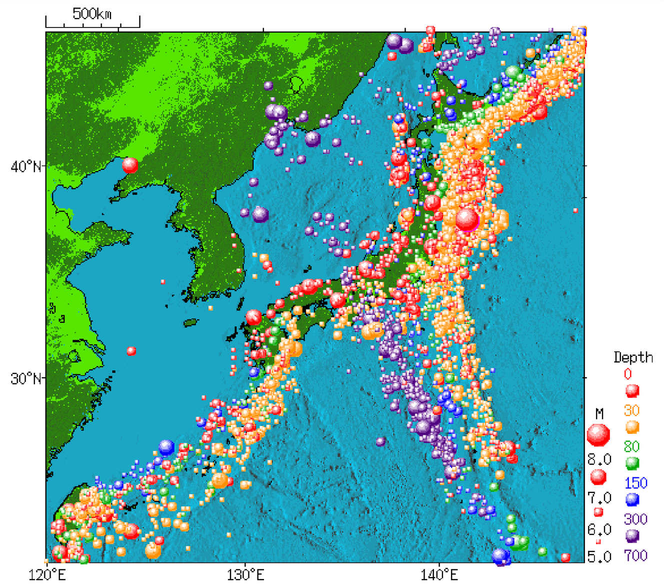

- More complete earthquake catalog for Japan and its surrounding regions
- JMA magnitude (Mj) has been converted to Mw (Uchide & Imanishi, 2018)

$$M_w = aM_j^2 + bM_j + c.$$

$a = 0.053 \pm 0.003$, $b = 0.33 \pm 0.02$, and $c = 1.68 \pm 0.03$

- JMA Earthquake Magnitude of Completeness (Mc ~ 3.3) much lower than CMT catalog (Mc ~ 5)
- Over two million earthquakes

Clustering Analysis with Unsupervised Machine Learning:

K-means Clustering

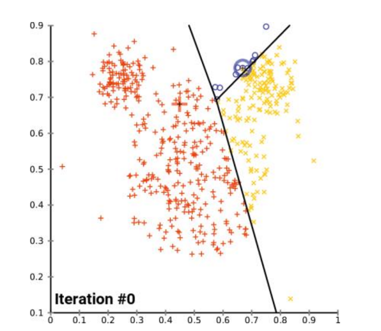

1. Initialize k random centroids
2. Create clusters
3. Recalculate the centroids
4. Repeat until convergence.

Silhouette Score

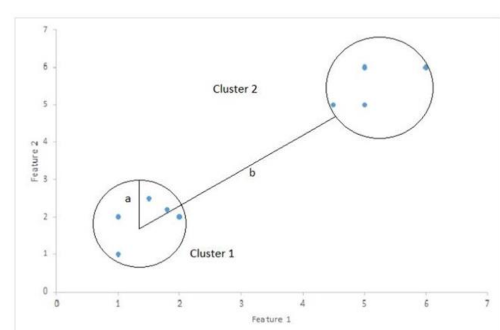

Silhouette Score = (b-a)/max(a,b)
a= average intra-cluster distance
b= average inter-cluster distance

Spectral Clustering

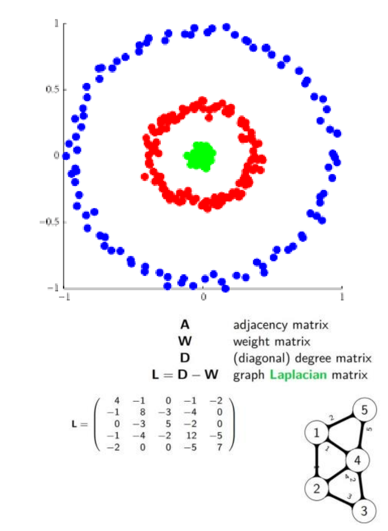

b-value analysis and its error analysis:

$$b_0 = \frac{1}{\ln(10)*(\mu - M_c)} \qquad \sigma_{b_0} = 2.3 b_0^2 \sqrt{\frac{\sum_{i=1}^{N}(M_i-\mu)^2}{N(N-1)}}$$

$$b_1 = \frac{1}{\ln(10)*(\mu - (M_c - \Delta M/2))} \qquad \sigma_{b_1} = 2.3 b_1^2 \sqrt{\frac{\sum_{i=1}^{N}(M_i-\mu)^2}{N(N-1)}}$$

$$b_2 = \frac{1}{\ln(10)*\Delta M} * \ln\left(1 + \frac{\Delta M}{\mu - M_c}\right) \qquad \sigma_{b_2} = \frac{\frac{\Delta M}{\mu - M_c}}{\ln(10)*\Delta M*\sqrt{N*(1+\frac{\Delta M}{\mu - M_c})}}$$

Gaussian Mixture Models Clustering

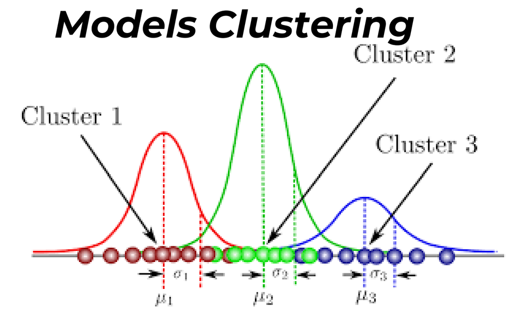

Mechanisms for the *b*-value Kinks

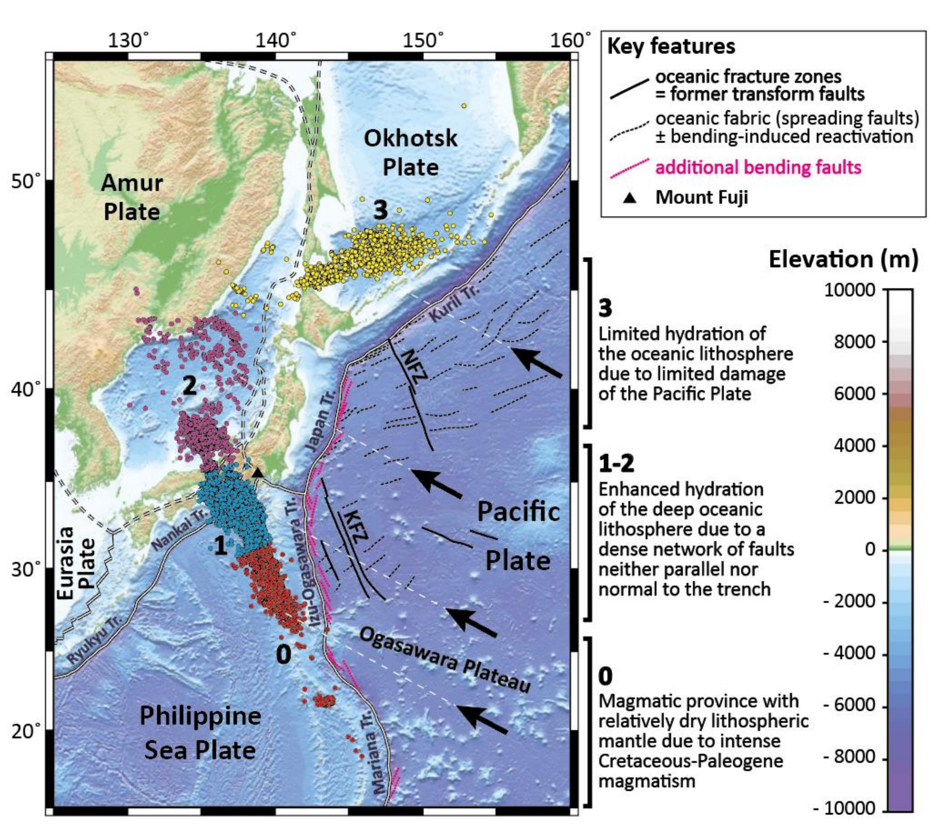

Pre-Subducting Plate Hydration Affects the Water Abundance in the MOW Halo.

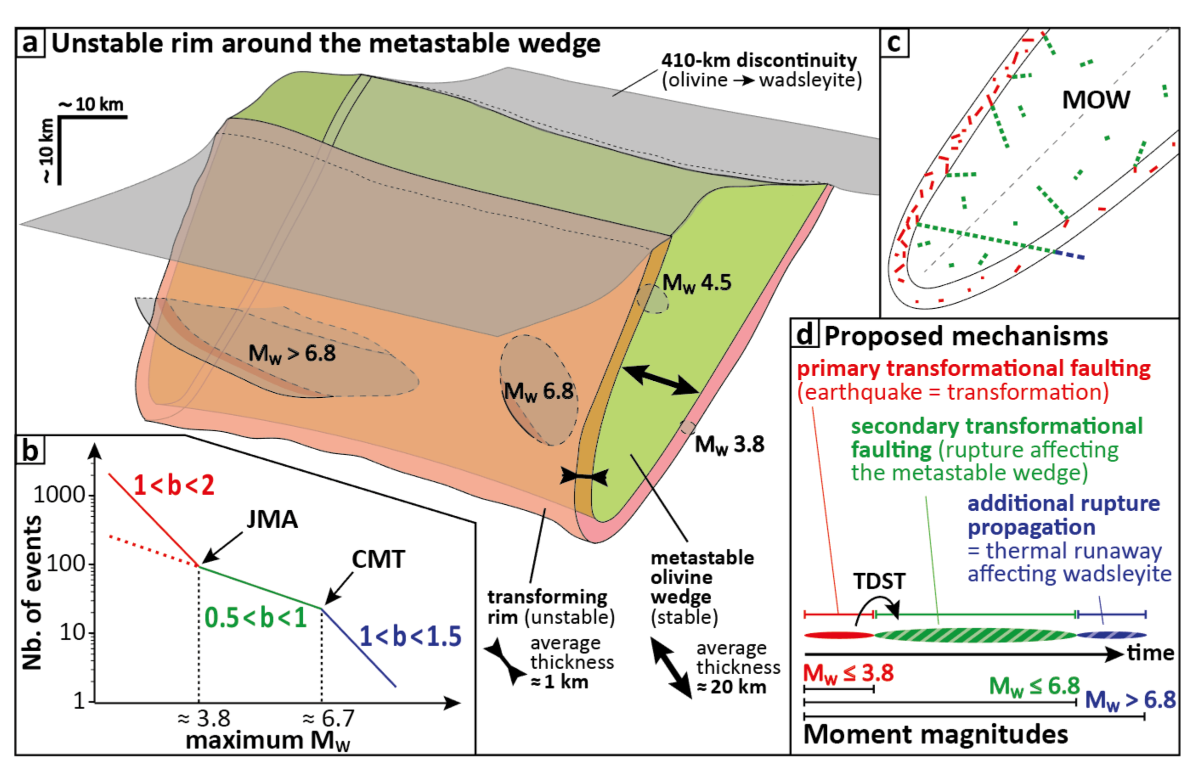

Deep-Focus Earthquakes Triggered in the Unstable Transforming Rim and can Propagate Into and then Outside the MOW. Water Acts as a Catalyst of Small Earthquakes in a Highly Reactive Halo of MOW.

References

1. Zhan, Z. Gutenberg–Richter law for deep earthquakes revisited: A dual-mechanism hypothesis. *Earth Planet. Sci. Lett.* **461**, 1–7 (2017).
2. Ishii, T. & Ohtani, E. Dry metastable olivine and slab deformation in a wet subducting slab. *Nature Geoscience* **14**, 526–530 (2021).
3. Warner., M. & Sandri, L., A review and new insights on the estimation of the b-value and its uncertainty. *Annals of Geophysics* **46**(6) (2003).
4. Ferrand, T. P. *et al.* Dehydration-driven stress transfer triggers intermediate-depth earthquakes. *Nature Communication* **8**, 1–11 (2017).

Results & Conclusion

K-means Clustering Analysis and *b*-value Analysis:

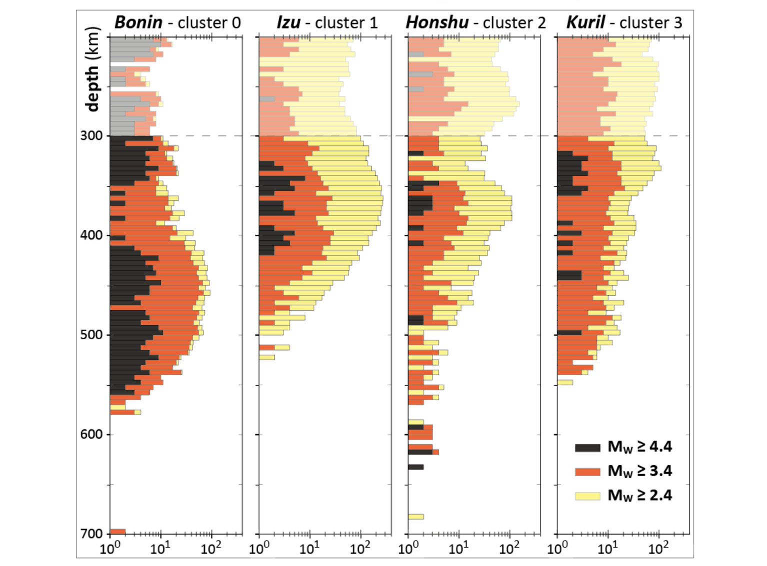

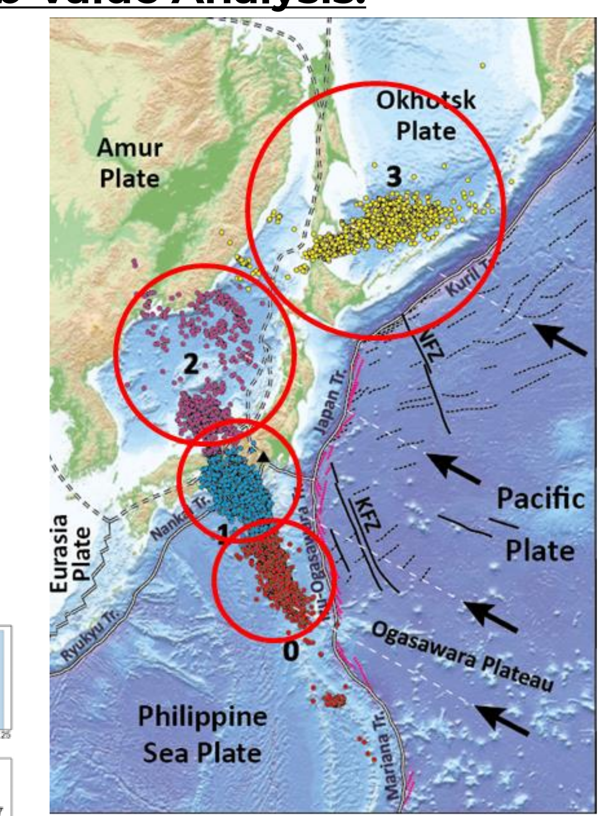

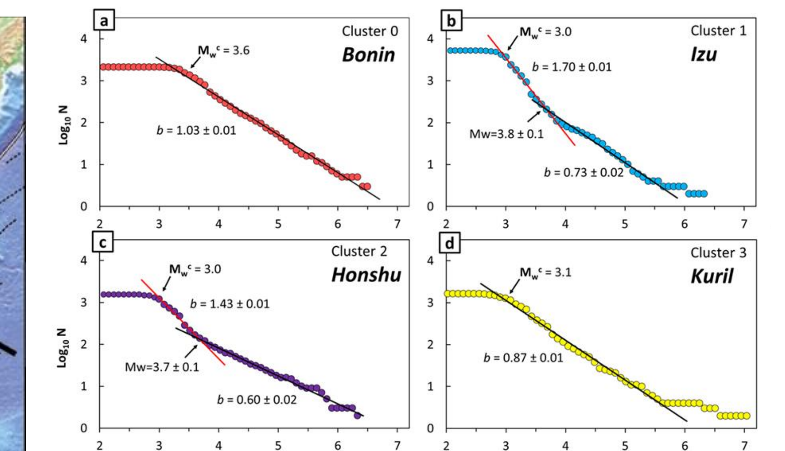

Table 1. *b* values and the standard deviations from three measurements

Region	b_0	σ_{b_0}	b_1	σ_{b_1}	b_2	σ_{b_2}
Kuril	0.97	0.01	0.87	0.01	0.92	0.01
Honshu*	1.72	0.02	1.43	0.01	1.57	0.01
Honshu**	0.65	0.02	0.60	0.02	0.62	0.02
Izu*	2.11	0.01	1.70	0.01	1.89	0.01
Izu**	0.80	0.03	0.73	0.02	0.77	0.02
Bonin	1.09	0.01	1.03	0.01	1.03	0.01

* Mw < 3.8
** Mw > 3.8
The b_0, b_1 and b_2 values are described in section 2.2.
The σ_{b_i} are the standard deviations for each distribution.

Silhouette Analysis: N =4

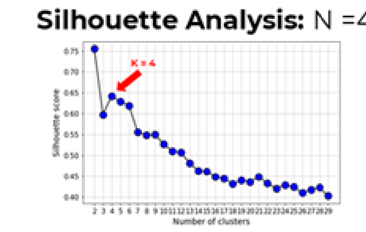

Bootstrapping

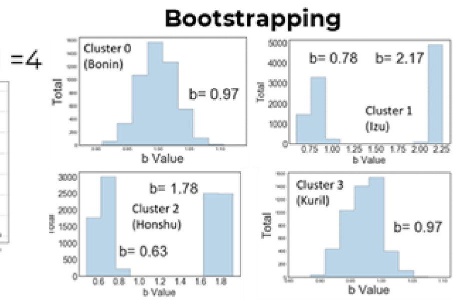

Mao et al. (in revision)

Spectral and GMM Clustering Analysis:

Table 2. *b* values and their errors from three measurements (Spectral Clustering, N=5)

Region	b_0	σ_{b_0}	b_1	σ_{b_0}	b_2	σ_{b_2}
Kuril	0.97	0.01	0.87	0.01	1.00	0.01
Honshu*	1.70	0.02	1.42	0.01	1.43	0.01
Honshu**	0.66	0.02	0.61	0.02	0.61	0.02
Izu*	2.10	0.01	1.69	0.01	1.71	0.01
Izu**	0.79	0.02	0.72	0.02	0.73	0.02
Bonin	0.93	0.01	0.84	0.01	0.95	0.01

Table 3. *b* values and their errors (Gaussian Mixture Models Clustering, N=4)

Region	b_0	σ_{b_0}	b_1	σ_{b_0}	b_2	σ_{b_2}
Kuril	0.97	0.01	0.87	0.01	0.88	0.01
Honshu*	1.70	0.02	1.42	0.01	1.43	0.02
Honshu**	0.65	0.02	0.61	0.02	0.61	0.02
Izu*	2.17	0.01	1.74	0.01	1.76	0.01
Izu**	0.83	0.03	0.76	0.02	0.76	0.03
Bonin	1.09	0.01	0.97	0.01	0.97	0.01

Comparison of Three Clustering Methods:

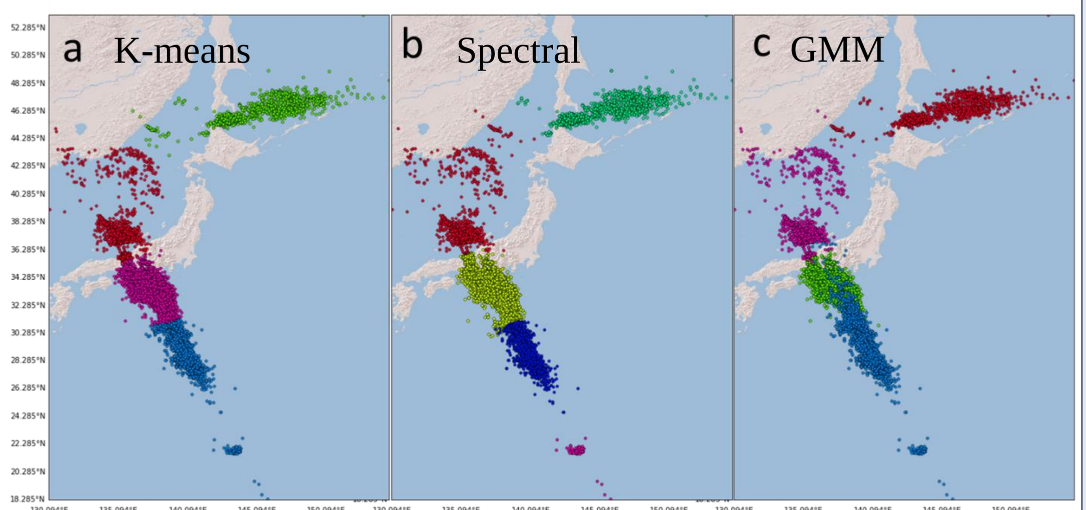

Three clustering methods generated similar clustering maps. The b-value analysis results are also similar. The clustering analysis of the JMA catalog is robust.

b-value analysis with CMT and IRIS catalogs :

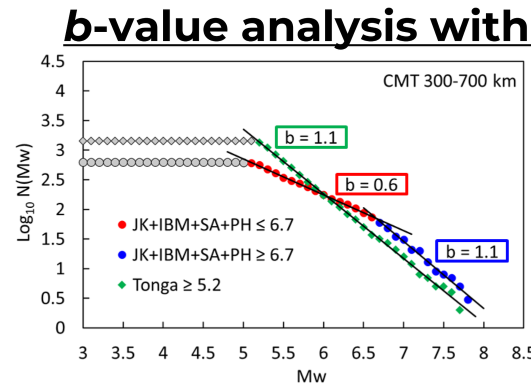

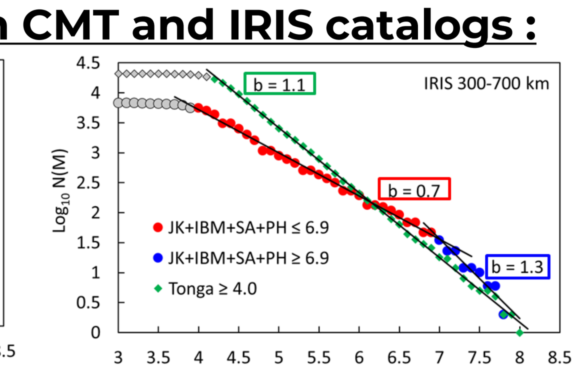

- IRIS and CMT catalogs show similar earthquake distributions
- Warm subduction zones show a change of b-values at Mw~6.8
- Cold Tonga subduction zone has a constant b-value of ~1.1

In JMA catalog, a new kink at Mw 3.8 was observed, in addition to the kink at Mw 6.5 in CMT and IRIS catalogs.

Two *b*-value Kinks indicate two different rupture dimension thresholds.

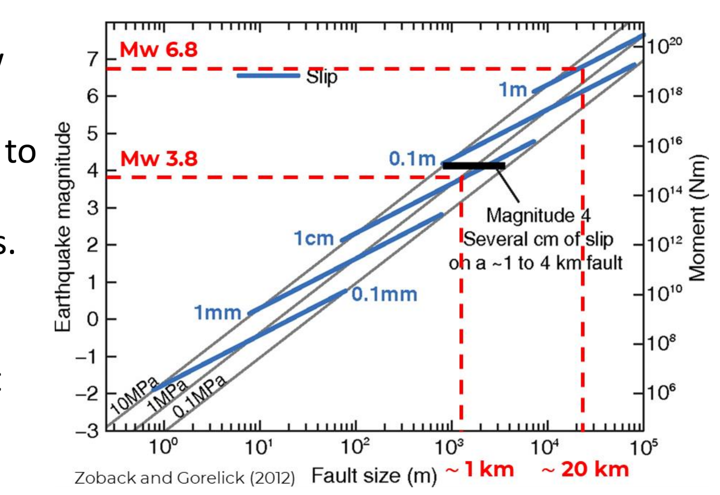

Conclusion:

- Unsupervised machine learning approaches facilitate the unbiased clustering of deep-focus earthquakes from the JMA catalog.
- The *b*-value kink at Mw~3.8 provides strong evidence for phase transformational faulting triggering deep-focus earthquakes in an unstable rim of the metastable olivine wedge with a width of ~1 km.
- In the highly reactive halo, water acts as a catalyst for transformational faulting, resulting in higher *b*-values in the Honshu and Izu slabs for Mw < 3.8.
- We speculate that the *b*-value kink at Mw~3.8 can be observed in other subduction zones with similar tectonic environments and earthquake catalogs.